J. Fluid Mech. (2014), *vol.* 745, *pp.* 398–408.
doi:10.1017/jfm.2014.111

Similarity solution for oblique water entry of an expanding paraboloid

G. X. Wu† and S. L. Sun

College of Shipbuilding Engineering, Harbin Engineering University, Harbin 150001, PR China

(Received 16 November 2013; revised 18 January 2014; accepted 24 February 2014;
first published online 19 March 2014)

Similarity solutions based on velocity potential theory are found to be possible in the case of an expanding paraboloid entering water when gravity is ignored. Numerical solutions are obtained based on the boundary element method. Iteration is used for the nonlinear boundary conditions on the unknown free surface, together with regular remeshing. Results are obtained for paraboloids with different slenderness (or bluntness). Flow features and pressure distributions are discussed along with the physical implications. It is also concluded that similarity solutions may be possible in more general cases.

Key words: waves/free-surface flows, wave–structure interactions

1. Introduction

Fluid–structure impact is a very common phenomenon in nature (e.g. violent wave or tsunami impact on offshore or coastal structures, ship slamming in rough seas, the landing of seaplanes) and has a wide range of practical applications. Extremely large fluid loading can be created during impact. In some cases, consequences can be catastrophic, causing loss of lives and wrecking of structures. Impact usually occurs within a very short period of time, over which both the fluid velocity and the fluid pressure change rapidly with time and location. This is accompanied by large and rapid deformation of the liquid surface. Such behaviour poses great challenges in fluid mechanics.

In most cases, fluid–structure impact based on velocity potential theory is a fully transient problem. In other words, the spatial and temporal variables in the mathematical analysis are fully independent, and the flow pattern and free-surface shape at one instant have no resemblance to those at another instant. However, there are many cases in which the flow is self-similar. When gravity is ignored under the condition of $W/g \gg T$, where W is the impact speed, g the acceleration due to gravity and T the time that the impact has lasted, well-known examples in two dimensions include those studied by Cumberbatch (1960) for a liquid wedge impacting on a flat wall and Dobrovol'skaya (1969) and Zhao & Faltinsen (1993) for a solid wedge entering a calm water surface. Other publications on two-dimensional (2D) problems

† Permanent address: Department of Mechanical Engineering, University College London, Torrington Place, London WC1E 7JE, UK. Email address for correspondence: g.wu@ucl.ac.uk

include the papers by Semenov & Iafrati (2006) for water entry of an asymmetric wedge, Xu, Duan & Wu (2008) for oblique water entry of an asymmetric wedge, Wu (2007) and Duan, Xu & Wu (2009) for impact between a liquid wedge and a solid wedge, and Semenov, Wu & Oliver (2013) on the impact of two liquid wedges. A related self-similar 2D problem is the one investigated by Keller, Milewski & Vanden-Broeck (2002), which involves the merging of two liquid wedges with the surface-tension effect. For axisymmetric cases, self-similar problems include the one studied by Shiffman & Spencer (1951) for water entry of a cone, through expanding the free-surface elevation into a series. This problem was also solved by Battistin & Iafrati (2003) and by Xu, Duan & Wu (2011). In three dimensions, Sun & Wu (2013*a*) considered the oblique water entry of a cone and subsequently (in Sun & Wu 2013*b*) solved the problem of water entry of non-axisymmetric bodies with varying speed.

While the above research on self-similar problems has provided significant insight into fluid–structure impact phenomena, the shapes of the solid surface in all these works are limited. In particular, the body surface has no curvature in two dimensions or, for three-dimensional (3D) problems, in the plane of a given azimuth of the cylindrical system, although some work has been done in the time domain, including the papers by Zhao & Faltinsen (1996) and Battistin & Iafrati (2003) for 2D problems, by Faltinsen & Zhao (1997) for an axisymmetric problem and by Korobkin & Scolan (2006) for a 3D problem. The present work considers the self-similar flow for a more general body shape, an expanding paraboloid entering water at a constant speed. Problems of this kind do not seem to have been solved. Part of the reason may be that the fluid flow generated by a rigid paraboloid entering a liquid surface is not self-similar, as there is no geometric similarity in the shapes of the body at different time steps. However, as we shall show in this paper, if the paraboloid expands in a prescribed way to achieve geometric similarity, self-similar flow can become possible. The solution of this problem can then provide some new insights into fluid–structure impact behaviour.

The problem of an expanding body considered here is not purely of mathematical interest. In fact, a well-known case in the free-surface flow problem is Dirichlet's ellipsoid (Lamb 1932, § 382). The expansion or contraction of a liquid ellipsoid in a prescribed way allows the analytical solution to be obtained in a simple explicit form. Such a solution has played a vital role in the free-surface flow problem. Longuet-Higgins (1976) also solved a family of self-similar problems for an expanding Dirichlet ellipse (Lamb 1932, § 382), a hyperbola and other shapes. The mathematical solutions were found to provide great insight into wave breaking (Longuet-Higgins & Cokelet 1976; Longuet-Higgins 1980, 1983*b*) and bubble busting through the free surface (Longuet-Higgins 1983*a*). A potential application of water entry of an expanding body is in the $2D + t$ theory for a ship (Faltinsen & Zhao 1991). When calculation starts from a 2D section at the bow and then continues along the ship length, it is equivalent to the body expanding. Such a practice has in fact been used by Tassin *et al.* (2013).

2. Mathematical model and numerical procedure

2.1. *The mathematical model*

The problem of an expanding paraboloid entering initially calm water obliquely with constant speed is sketched in figure 1. A Cartesian coordinate system with origin O and x_0, y_0 and z_0 axes fixed in space is defined, in which the x_0–y_0 plane lies on the undisturbed free surface and z_0 points vertically upwards. Here x_0 is defined along the

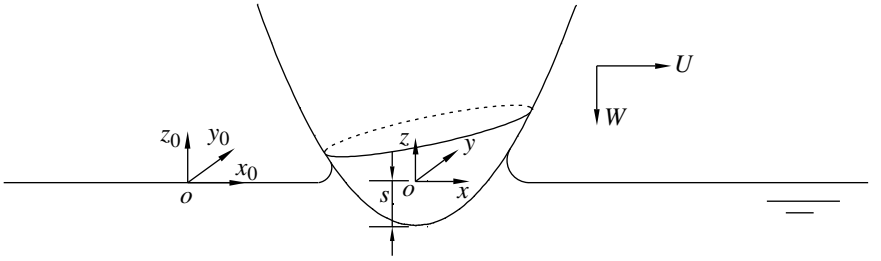

FIGURE 1. Sketch of the problem.

direction of the horizontal velocity U of the body, and W is the vertical downwards velocity of the body. The fluid is assumed to be incompressible on the basis of small Mach number and inviscid on the basis of small fluid–structure impact time. The flow can be irrotational with a velocity potential ϕ, as there is no initial vorticity. Thus, from the continuity equation we have

$$\nabla^2\phi = 0. \tag{2.1}$$

A Cartesian coordinate system with x, y and z axes formed by moving the x_0, y_0 and z_0 axes with the body at the same speed in the horizontal direction is also defined. Thus $x = x_0 - Ut$, $y = y_0$ and $z = z_0$. Within this coordinate system, the shape of the paraboloid may be written as

$$f(x, y, z, t) = x^2 + y^2 - \lambda s\,(z + s) = 0, \tag{2.2}$$

where $s = Wt$ and λ is a constant. This shows that, as well as moving with the translational velocity, the radius of the circular horizontal cross-section expands at the rate of $s^{1/2}$. On $f = 0$, (2.2) gives

$$\frac{\mathrm{d}f}{\mathrm{d}t} = 0, \tag{2.3}$$

or

$$n_x\frac{\mathrm{d}x_0}{\mathrm{d}t} + n_y\frac{\mathrm{d}y_0}{\mathrm{d}t} + n_z\frac{\mathrm{d}z_0}{\mathrm{d}t} = -\frac{f_t}{A} \tag{2.4}$$

where $\boldsymbol{n} = (n_x, n_y, n_z)$ is the normal of the surface pointing into the fluid domain and can be written as

$$n_x = f_x/A, \quad n_y = f_y/A, \quad n_z = f_z/A, \quad A = \sqrt{f_x^2 + f_y^2 + f_z^2}. \tag{2.5}$$

We note that the left-hand side of (2.4) is the normal velocity of the body surface, which must be equal to the fluid particle velocity in the same direction based on the impermeable kinematic condition. Thus

$$\frac{\partial\phi}{\partial\boldsymbol{n}} = -\frac{f_t}{A}. \tag{2.6}$$

On the free surface $z = \zeta$, the following dynamic and kinematic boundary conditions must be satisfied:

$$\phi_t - U\phi_x + \tfrac{1}{2}(\phi_x^2 + \phi_y^2 + \phi_z^2) = 0, \tag{2.7}$$

$$\zeta_t = \phi_z - \zeta_x(\phi_x - U) - \zeta_y\phi_y, \tag{2.8}$$

where the acceleration g due to gravity has been omitted from (2.7) on the basis of $W/g \gg T$, with T being the total impact time of interest.

2.2. *Self-similar solution*

As the body being considered is axisymmetric, it is convenient to introduce a polar coordinate system

$$x = r\cos\theta, \quad y = r\sin\theta. \tag{2.9}$$

We seek self-similar solutions of the form

$$\phi(x, y, z, t) = sW\varphi(\alpha, \theta, \beta), \quad \alpha = r/s,\ \beta = z/s. \tag{2.10}$$

Here, the temporal variable has been incorporated into α and β, and φ no longer depends explicitly on time in the new system. To ensure that such a solution is possible, it is necessary to verify that the governing equation and all the boundary conditions for φ do not contain s explicitly. This is clearly true for Laplace's equation in (2.1). In the new system, the body shape given by (2.2) becomes

$$\alpha^2 - \lambda(\beta + 1) = 0. \tag{2.11}$$

The body-surface boundary condition in (2.6) can be written as

$$\frac{\partial\varphi}{\partial \boldsymbol{n}} = \varepsilon\cos\theta n_\alpha - n_\beta - (\beta + 1)n_\beta \tag{2.12}$$

where $\varepsilon = U/W$ and

$$n_\alpha = \frac{2\alpha}{\sqrt{4\alpha^2 + \lambda^2}}, \quad n_\beta = -\frac{\lambda}{\sqrt{4\alpha^2 + \lambda^2}}. \tag{2.13}$$

The first two terms on the right-hand side of (2.12) represent the normal velocity caused by the translational motion of the body, and the last term denotes the contribution from the body expansion. In the new system, the dynamic and kinematic boundary conditions on the free surface, (2.7) and (2.8), can be written as

$$\varphi - \alpha\varphi_\alpha - \beta\varphi_\beta = \varepsilon\cos\theta\varphi_\alpha - \varepsilon\sin\theta\varphi_\theta/\alpha - [\varphi_\alpha^2 + (\varphi_\theta/\alpha)^2 + \varphi_\beta^2]/2, \tag{2.14}$$

$$\beta - \alpha\beta_\alpha = \varphi_\beta - (\varphi_\alpha - \varepsilon\cos\theta)\beta_\alpha - (\varphi_\theta/\alpha + \varepsilon\sin\theta)\beta_\theta/\alpha. \tag{2.15}$$

Far away from the body, the fluid is assumed to be undisturbed and we have

$$\varphi \to 0, \quad \sqrt{\alpha^2 + \beta^2} \to \infty. \tag{2.16}$$

It can then be seen that the governing equation and all the boundary conditions on φ do not involve s explicitly. This demonstrates that a self-similar solution is possible for the case of an expanding paraboloid entering water.

2.3. *Solution procedure*

Through Green's identity, the differential equation in (2.1) can be converted to the integral form

$$A(p)\varphi(p) = \int\left[\frac{1}{R_{pq}}\frac{\partial\varphi(q)}{\partial n_q} - \varphi(q)\frac{\partial}{\partial n_q}\left(\frac{1}{R_{pq}}\right)\right]\mathrm{d}s_q, \tag{2.17}$$

where $A(p)$ is the solid angle at point p on the surface of the fluid domain and R_{pq} is the distance between points p and q. The integration is performed over the whole boundary of the fluid domain, including the free surface, the body surface and the control surface away from the body. These surfaces are discretized into many small elements, and φ is approximated by a shape function in each element (Sun & Wu 2013*a*). We note that the shape of the free surface on which the conditions (2.14) and (2.15) are imposed is unknown before obtaining the solution. One obvious way to resolve this issue is to use an iteration method. We can start with $\varphi = 0$ on the undisturbed free surface, or $\beta = 0$. Using the potential φ on the free surface and the normal velocity φ_n on the body surface, (2.17) can be solved to obtain the unknown φ_n on the free surface and φ on the body surface. Then the free surface together with the potential there can be updated by using (2.14) and (2.15) in an integral form similar to that used by Wu, Sun & He (2004) for a 2D problem. Remeshing is applied if the elements have been significantly distorted (Sun & Wu 2013*b*). Equation (2.17) is then solved again. The process is continued until convergence has been achieved based on the pressure

$$C_p = -2\varphi + 2\alpha\varphi_\alpha + 2\beta\varphi_\beta + 2\varepsilon\cos\theta\varphi_\alpha - 2\varepsilon\sin\theta\varphi_\theta/\alpha - \nabla\varphi\cdot\nabla\varphi, \tag{2.18}$$

which is non-dimensionalized by $\rho W^2/2$, where ρ is the density of the fluid.

3. Numerical results and discussions

3.1. *Verification through a convergence study and comparison for a cone*

We first consider the problem of a cone entering water. The cone's surface can be written as

$$f(x, y, z, t) = \sqrt{x^2 + y^2} - \lambda(z + s) = 0, \tag{3.1}$$

or

$$\alpha - \lambda(\beta + 1) = 0. \tag{3.2}$$

This gives

$$n_\alpha = \frac{1}{\sqrt{1+\lambda^2}}, \quad n_\beta = -\frac{\lambda}{\sqrt{1+\lambda^2}}, \quad n_\theta = 0. \tag{3.3}$$

Because the cone is not undergoing expansion, the last term of the body-surface boundary condition in (2.12) should be dropped while the normal components are replaced by those in (3.3).

Figure 2 panels (*a*) and (*b*) show, respectively, the free-surface elevation of and pressure on the cone, obtained with different meshes. The smallest element is used around the jet root defined on the free surface with the largest curvature shown in figure 2(*a*). Its size then increases at a rate of 1.02 away from the jet root. The meshes used to obtain these results correspond to the smallest element sizes of 0.02, 0.04 and 0.06. The deadrise angle, defined as the angle between the cone surface and the undisturbed free surface, is $\pi/3$, which corresponds to $\tan^{-1}(\lambda) = \pi/6$. The results for vertical entry obtained from these three meshes are in good agreement. Figure 3 panels (*a*) and (*b*) show further comparisons of the results for oblique entry obtained from the present similarity solution with a mesh size of 0.04 and those given by the time domain solution of Sun & Wu (2013*a*). Good agreement can be observed.

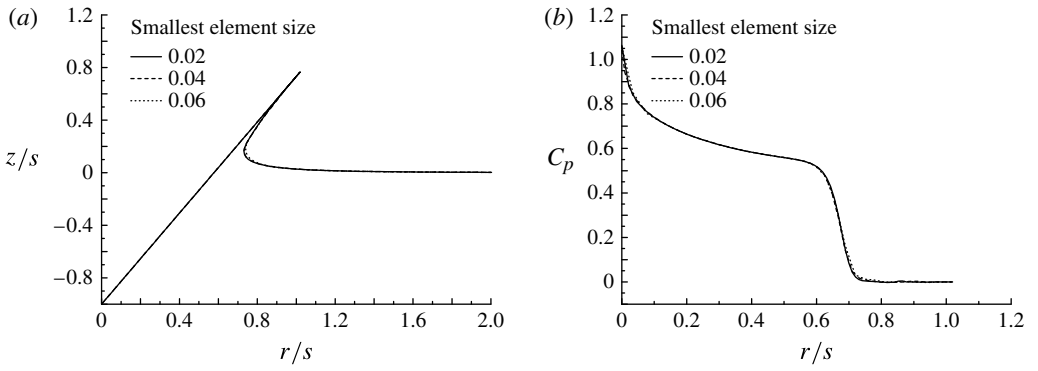

FIGURE 2. Convergence study using different meshes for vertical entry of a cone into water, with $\lambda = \tan(\pi/6)$: (*a*) free-surface elevation of the cone; (*b*) pressure on the cone.

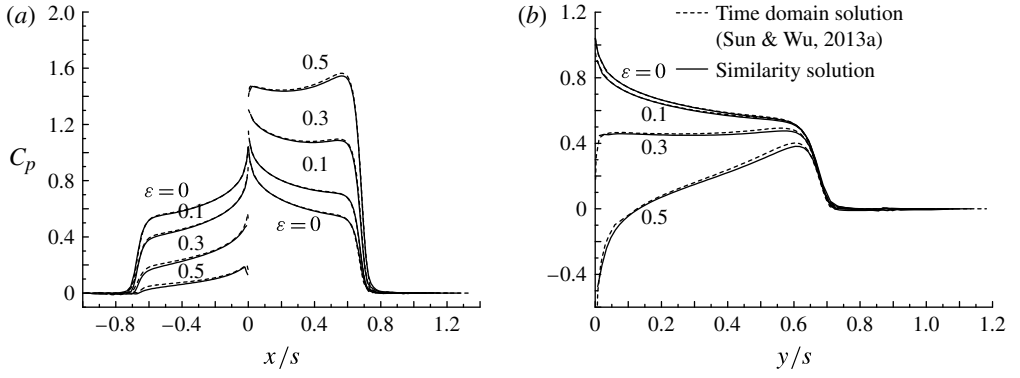

FIGURE 3. Pressure on the cone, with $\lambda = \tan(\pi/6)$, at (*a*) $y = 0$ and (*b*) $x = 0$.

3.2. *Water entry of an expanding paraboloid*

3.2.1. *Vertical water entry*

To consider vertical entry, we first take $\varepsilon = 0$ in (2.12), and then θ will not affect the results. To gain some insight into the variation of C_p along the body surface, we introduce at each point a local coordinate system (ξ, η), with axes perpendicular and tangential to the body surface, respectively, such that

$$\xi = \alpha n_\alpha + \beta n_\beta, \quad \eta = -\alpha n_\beta + \beta n_\alpha. \tag{3.4}$$

Equation (2.18) can be written as

$$C_p = -2\varphi + 2\xi\varphi_\xi + 2\eta\varphi_\eta - \nabla\varphi \cdot \nabla\varphi. \tag{3.5}$$

Thus

$$\frac{\partial C_p}{\partial \eta} = 2(\xi - \varphi_\xi)\varphi_{\eta\xi} + 2(\eta - \varphi_\eta)\varphi_{\eta\eta}. \tag{3.6}$$

Equations (2.11) and (2.12) give

$$\xi = \varphi_\xi \tag{3.7}$$

on the body surface. Thus, from (3.6), the tangential derivative of pressure at a point (ξ, η) on the body surface can be written as

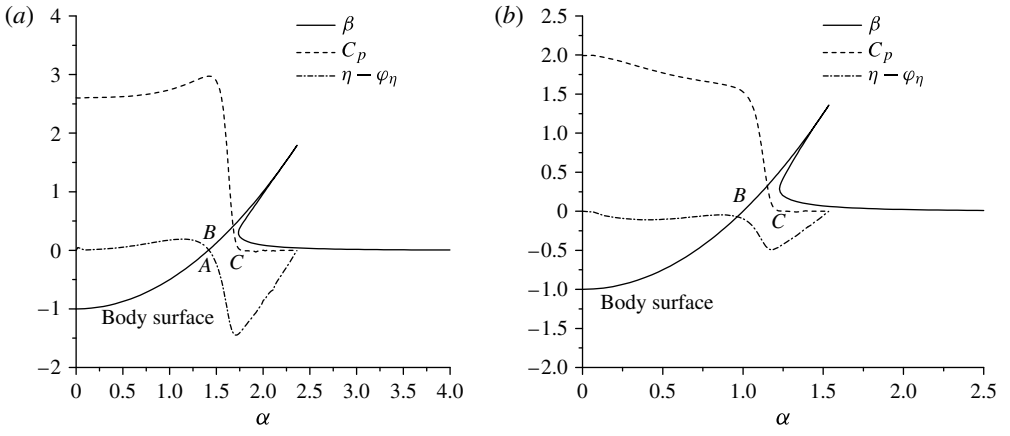

FIGURE 4. Variations of β, C_p and $\eta-\varphi_\eta$, in the cases where (*a*) $\lambda=2$, (*b*) $\lambda=1$.

$$\frac{\partial C_p}{\partial \eta}=2(\eta-\varphi_\eta)\varphi_{\eta\eta}. \tag{3.8}$$

For this axisymmetric case with $\varepsilon=0$, the free-surface boundary condition in (2.15) can also be written as

$$\eta-\xi\eta_\xi=\varphi_\eta-\varphi_\xi\eta_\xi. \tag{3.9}$$

On the intersection of the body surface with the free surface, (3.7) and (3.9) can be combined. This gives

$$\eta=\varphi_\eta. \tag{3.10}$$

Equations (3.7) and (3.10) mean that $\varphi_\alpha=\alpha$ and $\varphi_\beta=\beta$, the same as the relations in (2.11) of Semenov *et al.* (2013), which were obtained based on an argument involving the distance moved by the particle initially at the tip of the body to the intersection. Equation (3.8) gives $\partial C_p/\partial\eta=0$ at the free-surface and body-surface intersection as well as at the lowest point of the paraboloid with $\alpha=0$, i.e. the tip, as $\eta=\varphi_\eta$ there. These are the local extremum points of the pressure. However, as C_p is at the intersection, it is unlikely to be the global maximum point. The tip of the body, where $C_p=-2\varphi+1$ after the conditions $\varphi_\alpha=0$ and $\varphi_\beta=-1$ are applied, could be the global maximum point, depending on whether $\partial C_p/\partial\eta=0$ is satisfied on other parts of the body surface.

Results for the variations of $\eta-\varphi_\eta$ and C_p when $\lambda=2$ along the body surface are given in figure 4(*a*). It can be observed that there is a point with $\eta=\varphi_\eta$, marked by *A*. Correspondingly, there is a local pressure peak, which in fact is the global maximum. Notice that the intersection of the undisturbed free surface, i.e. $\beta=0$, with the body surface is at $\alpha=\sqrt{\lambda}=\sqrt{2}$. It is interesting to see that this point, marked by *B*, is roughly where the horizontal coordinate of point *A* is. We further note that for the point marked by *C*, which is the location corresponding to the point on the free surface with the lowest α value, its tangential direction is parallel to the β axis. The figure shows that the points *A*, *B* and *C* are close to each other. Around this region, the pressure changes rapidly, and beyond this region towards the intersection with the

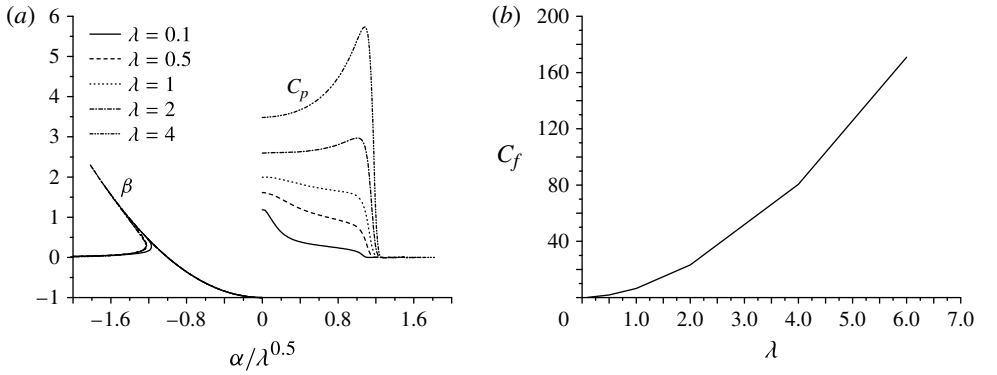

FIGURE 5. Water entry of paraboloids with different λ: (*a*) free-surface elevation and pressure C_p; (*b*) the force coefficient C_f.

free surface, the pressure is nearly zero. Physically, when the body enters water, point B has to move up but its path is blocked by the body, so it has to move away and also do a sharp turn to move along the body surface. This causes a large local pressure gradient. When the fluid turns, it moves with large velocity along the body surface but in a thin layer. The pressure across the thin layer varies little, and the pressure on the body surface and that on the free surface are almost the same.

The results for $\lambda = 1$ are given in figure 4(*b*). The body in this case is less blunt, and it is expected that the impact will be less severe, as demonstrated by the pressure curve which is lower in this figure than in figure 4(*a*). In particular, no inner point with $\eta = \varphi_\eta$ is observed. The global maximal pressure occurs at the tip of the body. However, similar to the case of $\lambda = 2$, the pressure drops rapidly around the region of points B and C and is nearly zero beyond this region.

Figure 5(*a*) gives the pressure distribution on the body surface and free-surface elevation for different λ values. Notice that the focus of the paraboloid is at $\lambda/4 - 1$. As λ decreases, the body will become more slender and the normal velocity of the body surface becomes smaller because of the smaller magnitude of n_β in (2.13). The pressure is therefore expected to be smaller, as can be seen in figure 5(*a*). However, (2.13) also shows that $n_\beta = -1$ at $\alpha = 0$, i.e. at the tip of the body, which is independent of λ. This suggests that away from the tip, the magnitude of n_β changes more quickly when λ is smaller. This leads to a more rapid change of pressure near the tip, as shown in figure 5(*a*). At the tip, however, the slopes of the pressure curves for all λ are zero, as discussed in (3.8). This differs from the results for a cone shown in figure 2(*b*), where the slope of the pressure curve at the tip is very steep, clearly caused by the discontinuity in the normal to the body surface at this point. The vertical force coefficient C_f in figure 5(*b*) is defined as

$$C_f = \int C_p n_\beta \, \mathrm{d}s. \tag{3.11}$$

It increases rapidly with λ.

3.2.2. *Oblique water entry*

If the paraboloid enters water obliquely, the problem is no longer axisymmetric and becomes a fully 3D problem. Figure 6 panels (*a*) and (*b*) show the free-surface

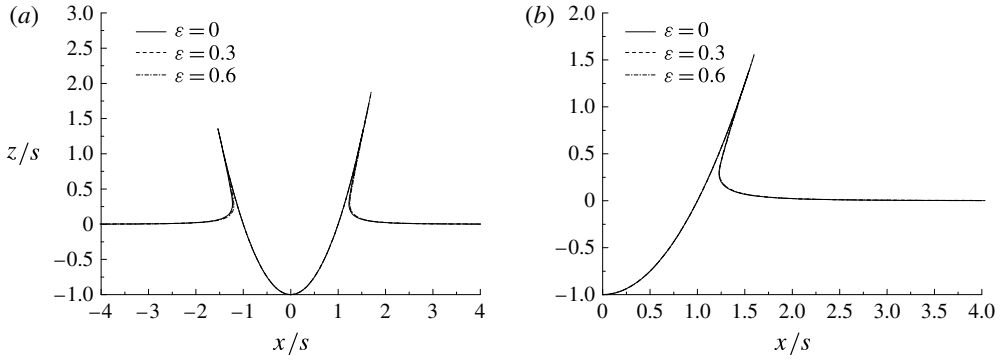

FIGURE 6. Free-surface elevation for the $\lambda = 1$ case: (a) in the $y = 0$ plane; (b) in the $x = 0$ plane.

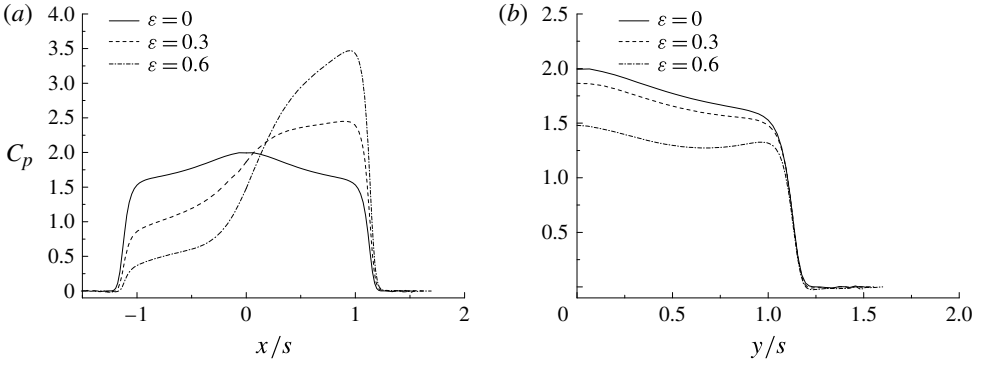

FIGURE 7. Pressure on the body surface for the $\lambda = 1$ case: (a) in the $y = 0$ plane; (b) in the $x = 0$ plane.

profiles in the planes $y = 0$ and $x = 0$, respectively, and figure 7 panels (a) and (b) plot the pressure for the paraboloid with $\lambda = 1$. These figures show that the effect of the horizontal velocity on the free-surface elevation is much smaller than the effect on the pressure. Due to the horizontal velocity in the x direction, the slope of the pressure curve in the $y = 0$ plane is no longer zero at the tip, as shown in figure 7(a), while it is still zero in the $x = 0$ plane, clearly because of the symmetry about the $y = 0$ plane. In contrast to the discontinuity and sharp variation at the tip of a cone (Sun & Wu 2013*a*), the pressure here is finite and continuous at the tip. In the vertical entry case, the peak pressure for $\lambda = 1$ is at the tip of the body, as shown in figure 5(a). When there is a horizontal velocity and water is being pushed away by the body surface, the counter-action of the water leads to a pressure increase on the front side and the peak pressure moves away from the tip, as shown in figure 7(a). Correspondingly, the pressure on the back side decreases.

Figure 8 plots the 3D pressure contours on the body surface. For vertical entry with $\varepsilon = 0$ in figure 8(a), the contours are all circular lines as the problem is axisymmetric. The peak is at the tip, and the pressure decreases as the radius of the circle increases for the case of $\lambda = 1$. With $\varepsilon = 0.3$ or 0.6, the centre of the curve has been pushed to the right and all the circles have been twisted. Near the centre the curves are very dense on the front side, indicating a larger pressure gradient. Moving along the curve

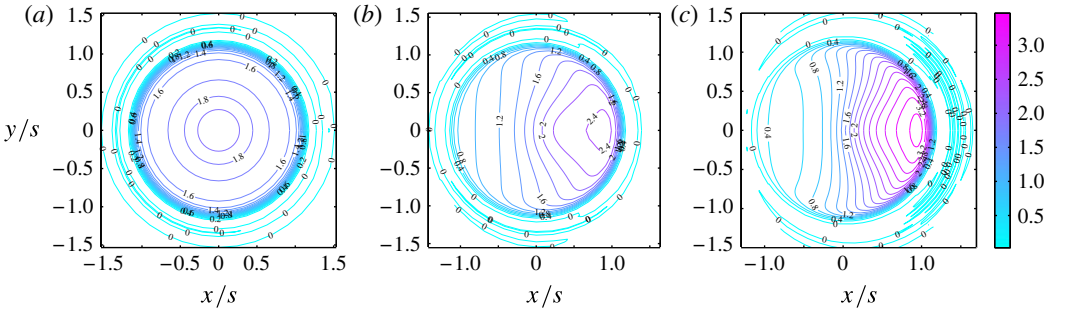

FIGURE 8. Pressure contours on the body surface, for $\lambda = 1$, with (*a*) $\varepsilon = 0$; (*b*) $\varepsilon = 0.3$; (*c*) $\varepsilon = 0.6$.

to the back side, the curves become less and less dense, and the pressure gradient becomes smaller and smaller. All these features become more evident as the horizontal velocity increases, as shown in figure 8(*c*).

4. Conclusions

Self-similar solutions are found to be possible for entry of a body with curvature into water if the body expands in an appropriately prescribed way. Numerical solutions have been obtained for an expanding paraboloid entering water. It has been found that for vertical entry of a slender body, the pressure peaks at the tip of the body and then drops rapidly away from the tip. As the body becomes less slender, the pressure at the tip increases but its gradient drops; more importantly, the peak pressure moves away to a location close to the intersection point of the undisturbed free surface and the body surface. Near this intersection, the vertical path of the fluid is blocked. The flow is pushed away and turns sharply along the direction of the body surface. This leads to a very large pressure gradient. Beyond that region, the pressure on the body surface is nearly zero. In the case of oblique entry, the circular shape of the pressure contour is destroyed. As the horizontal velocity increases, a new pressure-peak centre will form. The contour is highly dense on the front side of the peak and becomes less dense as one walks along a pressure line towards the back side.

Acknowledgements

This work was supported by Lloyd's Register Foundation (LRF) through the joint centre involving University College London, Shanghai Jiaotong University and Harbin Engineering University, to which the authors are most grateful. LRF supports the advancement of engineering-related education, and funds research and development that enhances safety of life at sea, on land and in the air.

This work was also supported by the National Natural Science Foundation of China (grant nos 11302057 and 11302056).

REFERENCES

BATTISTIN, D. & IAFRATI, A. 2003 Hydrodynamic loads during water entry of two-dimensional and axisymmetric bodies. *J. Fluids Struct.* **17**, 643–664.

CUMBERBATCH, E. 1960 The impact of a water wedge on a wall. *J. Fluid Mech.* **7**, 353–374.

DOBROVOL'SKAYA, Z. N. 1969 On some problems of similarity flow of fluid with a free surface. *J. Fluid Mech.* **36**, 805–829.

DUAN, W. Y., XU, G. D. & WU, G. X. 2009 Similarity solution of oblique impact of wedge-shaped water column on wedged coastal structures. *Coast Engng* **56**, 400–407.

FALTINSEN, O. & ZHAO, R. 1991 Numerical predictions of ship motions at high forward speed. *Phil. Trans. R. Soc. Lond.* A **334**, 241–252.

FALTINSEN, O. & ZHAO, R. 1997 Water entry of ship sections and axisymmetric bodies. In *AGARD FDP and Ukraine Institute of Hydromechanics Workshop on 'High Speed Body Motion in Water'*.

KELLER, J. B., MILEWSKI, P. A. & VANDEN-BROECK, J.-M. 2002 Breaking and merging of liquid sheets and filaments. *J. Engng Maths* **42**, 283–290.

KOROBKIN, A. A. & SCOLAN, Y.-M. 2006 Three-dimensional theory of water impact. Part 2. Linearized Wagner problem. *J. Fluid Mech.* **549**, 343–373.

LAMB, H. 1932 *Hydrodynamics*. 6th edn. Cambridge University Press.

LONGUET-HIGGINS, M. S. 1976 Self-similar, time-dependent flows with a free surface. *J. Fluid Mech.* **73**, 603–620.

LONGUET-HIGGINS, M. S. 1980 On the forming of sharp corners at a free surface. *Proc. R. Soc. Lond.* A **371**, 453–478.

LONGUET-HIGGINS, M. S. 1983*a* Bubbles, breaking waves and hyperbolic jets at a free surface. *J. Fluid Mech.* **127**, 103–121.

LONGUET-HIGGINS, M. S. 1983*b* Rotating hyperbolic flow: particle trajectories and parametric representation. *Q. J. Mech. Appl. Maths* **36**, 247–270.

LONGUET-HIGGINS, M. S. & COKELET, E. D. 1976 The deformation of steep surface waves on water. I. A numerical method of computation. *Proc. R. Soc. Lond.* A **350**, 1–26.

SEMENOV, Y. A. & IAFRATI, A. 2006 On the nonlinear water entry problem of asymmetric wedges. *J. Fluid Mech.* **547**, 231–256.

SEMENOV, Y. A., WU, G. X. & OLIVER, J. M. 2013 Splash jet generated by collision of two liquid wedges. *J. Fluid Mech.* **737**, 132–145.

SHIFFMAN, M. & SPENCER, D. C. 1951 The force of impact on a cone striking a water surface (vertical entry). *Commun. Pure Appl. Maths* **4**, 379–417.

SUN, S. L. & WU, G. X. 2013*a* Oblique water entry of a cone by a fully three-dimensional nonlinear method. *J. Fluids Struct.* **42**, 313–332.

SUN, S. L. & WU, G. X. 2013*b* Oblique water entry of non-axisymmetric bodies at varying speed by a fully nonlinear method. *Q. J. Mech. Appl. Maths* **66**, 366–393.

TASSIN, A., PIRO, D. J., KOROBKIN, A. A. & COOKER, M. J. 2013 Two-dimensional water entry and exit of a body whose shape varies in time. *J. Fluids Struct.* **40**, 317–336.

WU, G. X. 2007 Two-dimensional liquid column and liquid droplet impact on a solid wedge. *Q. J. Mech. Appl. Maths* **60**, 497–511.

WU, G. X., SUN, H. & HE, Y. S. 2004 Numerical simulation and experimental study of water entry of a wedge in free fall motion. *J. Fluids Struct.* **19**, 277–289.

XU, G. D., DUAN, W. Y. & WU, G. X. 2008 Numerical simulation of oblique water entry of an asymmetrical wedge. *Ocean Engng* **35**, 1597–1603.

XU, G. D., DUAN, W. Y. & WU, G. X. 2011 Numerical simulation of water entry of a cone in free fall motion. *Q. J. Mech. Appl. Maths* **64**, 265–285.

ZHAO, R. & FALTINSEN, O. 1993 Water entry of two-dimensional bodies. *J. Fluid Mech.* **246**, 593–612.

ZHAO, R. & FALTINSEN, O. 1996 Water entry of arbitrary two-dimensional sections with and without flow separation. In *Twenty-First Symposium on Naval Hydrodynamics* pp. 408–425. The National Academies Press.